

Graphene Oxide/L-phenylalanine/polymethacrylamide Nanocomposite as an Efficient Fluorescent Nanosensor for Heavy Metals Detection in Aqueous Media

Mehdi Barzegarzadeh

Tabriz University: University of Tabriz

Mohammad Sadegh Amini-Fazl (✉ ms.amini@tabrizu.ac.ir)

Tabriz University: University of Tabriz <https://orcid.org/0000-0002-6330-5333>

Seyed Yasin Yazdi-Amirkhiz

Tehran University of Medical Sciences

Original Article

Keywords: Graphene oxide, Heavy metal detection, RAFT, L-phenylalanine, Nanosensor

Posted Date: February 12th, 2021

DOI: <https://doi.org/10.21203/rs.3.rs-186494/v1>

License: © ⓘ This work is licensed under a Creative Commons Attribution 4.0 International License.

[Read Full License](#)

Abstract

The application and fabrication of graphene-based nanomaterials have, caught great attention in the field of sensors in recent years. In this study, a graphene oxide (GO)-based heavy metals nanosensor was prepared *via* the surface reversible addition-fragmentation chain transfer (RAFT) method. First, GO was prepared from graphene and was modified with *L*-phenylalanine (LP). Then a RAFT agent was attached chemically into the surface of GO-LP. Next, GO-LP/polymethacrylamide (GO-LP/PMAM) was prepared *via* the polymerization of methacrylamide (MAM) monomers on the surface of the GO. The surface morphology and chemical properties of the prepared materials were examined by FT-IR, SEM, TGA, UV and PL techniques. The results of PL indicated that the PL intensity of GO-LP/PMAM compared to GO and GO-LP spectra in the water was stronger. Finally, the modified GO was employed as an excellent nanosensor for the selective detection of Cu (II) ions in the range of 0.25-2 mM (correlation coefficient R^2 0.9903). Absence any obvious alteration in the fluorescence intensity after the addition of other metal ions indicated the great selectivity for Cu (II). Based on the experimental results, the surface-functionalized GO with RAFT strategy could be successfully employed as a promising nanosensor for selective detecting of Cu (II) ions.

1. Introduction

Toxic heavy metal ions in the environment are detrimental hazards to aquatic ecosystems and human life. Among such metal ions, the Cu^{2+} is a particularly important divalent cation that plays a critical role as a catalytic cofactor for a variety of metalloenzymes, including superoxide dismutase, cytochrome c oxidase, tyrosinase and nuclease [21]. However, under overloading conditions, copper exhibits toxicity and can cause oxidative stress and disorders associated with neurodegenerative diseases (e.g. Alzheimer's and Wilson's diseases) [15]. Hence, designing and developing innovative materials for simple, sensitive and rapid monitoring and sensing of heavy metals is necessary, even in trace amounts [6, 7, 24]. In this respect, enormous efforts have been dedicated to develop analytical methods for the detection of heavy metal ions [24, 9]. Yet, the most common techniques, e.g., atomic emission spectrometry, atomic absorption spectrometry and X-ray fluorescence spectrometry are still suffering from the time-consuming process, expensive instruments, and intensive labor. To overcome these problems, different means of colorimetric, optical, and electrochemical platforms have been broadly investigated for the installation of simple, sensitive, selective, and cost-effective approaches [22, 16]. More attempts have been particularly dedicated to the progress of smart and innovative fluorophores for heavy metal ions detection. Despite these efforts, there are still plenty of challenges with fabricating and developing a cost-effective and highly selective and sensitive chemo-sensor for monitoring heavy metal ions. The optical methods based on graphene-based nanosensors have recently been proposed as one of the promising methods for the detection of heavy metal ions owing to their potential benefits of easy design and sensitive recognition of metal ions [4].

The graphene oxide presents a unique feature such as easy functionalization, high electronic conductivity, large specific surface area, exclusive optical properties, chemical stability, and mechanical

and photonic properties that deliver a talented platform for the construction and design of innovative nanomaterials. In addition, graphenes as rapidly developing nanomaterials have attracted great attention owing to their possible applications in clinical medicine, biomedical field, and in sensors particularly in electrochemical sensors and fluorescence sensors.

Graphen usually does not have fluorescence property but through surface modification by some materials it can cause fluorescence [28, 2]. Typically, these methods can be categorized into “grafting from” and “grafting to” strategy. “Grafting from” methods are talented to grow polymers on the surface of the support with adjustable grafting dimension and controlled functionality [9, 23, 18, 14]. In this regard, a diversity of methods, for instance, coupling reaction [26], surface-initiated controlled radical polymerization (SI-CRP) such as atom transfer radical polymerization (ATRP) and RAFT polymerization [1, 25] have been developed to functionalize GO.

Some recent studies [10, 20, 19] have reported heavy metal characterization through quenching the intensity of fluorescence. For instance, **Hua et al** [11] for determination of mercury in river utilized SiO_2 modified by graphene quantum dot CdTe.

The major objectives of the present study are to develop effective chelating groups on the surface of the GO for the sensing of heavy metal ions from the aqueous media. For this purpose, the design strategy of the nanosensor was motivated based on “grafting from” method through surface modification of GO with PMAM via RAFT polymerization strategy (Scheme 1). This polymeric material with amide functional groups on the surface of GO could be employed as an agent to complex and chelate heavy metal ions from the aqueous media [13]. Therefore, the potentiality of prepared GOLP/PMAM-hydrogel as an effective nanosensor for the detecting of heavy metal ions from aqueous media was investigated.

2. Experimental

2.1. Materials

Graphene (Merck, 99%), *L*-phenylalanine (LP, Sigma), methacrylamide (MAM, Sigma, 99%), Azobisisobutyronitrile (AIBN, Aldrich, 98%), and 4-Cyano-4-(phenylcarbonothioylthio) pentanoic acid (Sigma) were used as received. All other materials were obtained from Sigma and used without any purification.

2.2. Characterization

An FT-IR spectrophotometer (Tensor 27, Bruker) was used to record the spectra by KBr pellets. UV–Vis absorption spectra were performed on a Shimadzu 1700 Model UV–Vis spectrophotometer. To determine the morphology of samples, the scanning electron microscopy (SEM) (MIRA3 FEG-SEM Tescan, Czech) was used. The dynamic light scattering (DLS) was achieved with a DLS-ZP/Particle Sizer (Malvern model Nanotracc Wave (Microtracc) with 658 nm diode laser). Thermo-gravimetric analysis (TGA) was obtained on a thermal analyzer (Polymer Laboratories, TGA 1750) with a 10°C/min heating rate from 25 to 800 °C

under argon atmosphere. The photoluminescence (PL) spectra were recorded by a spectrofluorometric FP-750, Jasco, Japan.

2.3. Synthesis of GO

According to the reported procedure, GO was prepared by some modification [12]. Briefly, 1.0 g of graphene powder was added in a solution of 120 mL H₂SO₄ (98%) and 20 mL HNO₃ (65%) in an ice bath. Then, 6 g KMnO₄ was added and stirred at 50°C for 12 h. After cooling the reaction mixture to room temperature, 130 mL ice and 1 mL H₂O₂ (30%) were added. By centrifuging at 6000 rpm, the solid product was separated and washed with distilled water HCl (37%) and EtOH several times and was dried at 50°C.

2.4. Functionalization of GO with LP

In GO powder dispersion solution (1 g GO in 100 mL distilled water) was added 100 mL distilled water containing 3 g LP and 0.018 g NaOH and stirred for 24 h at 25°C. After treating the colloidal dispersion with ethanol, the resulting precipitate was washed thoroughly with H₂O/EtOH mixture and dried at 50°C.

2.5. Functionalization of GO-LP with RAFT agent

GO-LP (300 mg) was dispersed in 12 mL dichloromethane (DCM) under a nitrogen atmosphere and was stirred with an excess amount of thionyl chloride (12 ml) for 24 h at 80 °C. The GO-LP-COCl was washed with distilled tetrahydrofuran (THF) to prevent the hydrolysis of the -COCl functional groups. Then 300 mg of dried GO-PL-COCl was dispersed in the 100 DCM containing 20 mg RAFT agent, 4-Cyano-4-(phenylcarbonothioylthio) pentanoic acid, and an equimolar amount of triethylamine and then was stirred under a nitrogen atmosphere for 12h. Finally, the product was washed several times with DCM and THF and dried at 50°C.

2.6. Synthesis of GO-LP/PMAM

The GO-LP/PMAM was prepared *via* RAFT polymerization method through the growing polymer on the GO surface. Briefly, GO-LP-RAFT agent (200 mg) was ultrasonically dispersed for 10 min in 25 mL of THF, followed by the addition of MAM (400 mg, 4.7 mmol), and AIBN (30 mg, 1.8 mmol) as initiators. After three freeze-pump-thaw cycles, the polymerization was completed at 70°C (~ 8 h). The resultant was precipitated by adding water and after that was washed with water and dried at 50°C.

2.7. The process for the determination of heavy metal ions

The test solution contained 1700 µl deionized water, 100 µl solutions of nanosensor (3 mg/ml) and 200 µl of each metal ion solution (10 mM) was treated under excitation at 280 nm to fluorescence achievement.

3. Results And Discussion

3.1. FT-IR analysis

To study the banding interactions in GO before and after functionalization procedures, FT-IR measurement was employed. In the GO spectrum (Fig. 1A), owing to the presence of oxide functional groups during the oxidation process, the characteristic peak related to different types of functionalities in GO such as C-O, O-H, C-H, C = O bands of hydroxyl and carboxylic acid moieties respectively appeared at 1047, 3431, 3010, 1626 and 1710 cm^{-1} , which prove the oxidation process. In LP functionalized GO spectra, the peaks that approve the covalent functionalization of the GO by LP molecules are the presence of C = O stretching groups of amides, carboxylate salts, and stretching groups of OH and NH at the range of 1639, 1693 and 3431 cm^{-1} , respectively. The appearance of acyl halide absorption peaks at 1835 cm^{-1} in the functionalized GO-LP FT-IR spectrum and also decreasing the OH stretching group confirmed a successful acylation process. The FT-IR spectrum of GO-RAFT agent indicates the stretching vibrations of C-S, C = S, and C-O at the range of 599, 1008 and 1148 cm^{-1} , respectively. The presence of these characteristics in the GO-RAFT agent spectrum confirmed the successful preparation of the RAFT agent. In the FT-IR spectrum of GO-LP/PMAM, the stretching vibrations of C = O amide, -CH and NH groups in the polymer chain were observed at 1667, 2910 and 3291 cm^{-1} , respectively. These notable bands revealed the successful formation of PMAM onto the surface of GO backbones.

3.2. Morphological study

The morphology of prepared materials was studied through SEM microscopic method. The related images of GO and GO-LP/PMAM are shown in Fig. 2. The SEM image of GO presented crispy two-dimensional layers with roughness and wrinkles on the surface, which may be due to the functional groups (carboxyl, epoxy, ketone, and hydroxyl) created during the oxidation process (Fig. 2A). In the SEM image of GO-LP/PMAM, the existence of crustal layers indicates that the main structure of GO is retained during the polymerization process (Fig. 2B). After the polymerization of MAM, due to the linkage of the polymeric chains onto the GO, the uniformity of roughness was obtained at the surface of GO. This layer linkage structure of prepared GO-LP/PMAM makes it potentially useable as a nanosensor for detecting various ions.

3.3. DLS analysis

By using DLS measurement, the size of GO and GO-LP/PMAM were determined in aqueous solution. The average size of GO and GO-LP/PMAM were respectively found to be 134.8 and 153.7 nm (Fig. 2C and 2D). The increase in particle size is another evidence that the RAFT polymerization process successfully occurred onto the GO.

3.4. Thermal analysis

TGA analysis was used to investigate the thermal stability and quantity of the surface-functionalized GO. From room temperature to 800 °C under argon, GO-LP-RAFT and GO-LP/PMAM samples showed three distinct stages (Fig. 3a). First, a weight-loss below 150 °C related to the removal of water is due to the formation of the intra- and inter-molecular anhydride bonds and releasing of CO_2 by the decarboxylation process. The first weight loss observed for GO-RAFT and GO-LP/PMAM was 21% and 16% respectively. In the second stage (from 155 to 700 °C), the weight loss observed for GO-RAFT and GO-LP/PMAM was

about 30% and 40 % respectively, being due to the heat decomposition of RAFT and PMAM carboxyl and amid groups [27]. In addition, the loss of 16.1 and 8.4 % respectively for GO-RAFT and GO-LP/PMAM in the range from 700 to 900 °C is attributed to the breakage of a PMAM chain and the dehydroxylation of GO upon thermal treatment [5, 8]. Results from the TGA data indicated that the quantity of the polymerization of MAM (PMAM) onto the GO surface was about 10%.

3.5. UV-Vis study

UV-Vis study was performed in dispersion state to detect the modification of GO. Typical peaks of GO observed at the 233 and 310 nm are respectively related to the $\pi-\pi^*$ transitions of aromatic C = C and C = O bonds [3] (Fig. 3b). In the spectrum of the GO-LP and GO-LP/PMAM, a redshift can be seen from 233 to 248 and 265 nm, respectively. This phenomenon could be attributed to the functionalization process onto the GO. Moreover, due to the reaction of the lone pair of GO through functionalization, the shoulder peak in the 310 nm was not observed in the spectrum of GO-LP and GO-LP/PMAM.

3.6. PL study

Figure 4 shows the PL spectra for GO, GO-LP, and GO-LP/PMAM with 4 mg/mL concentration in deionized water, which was used to study the quantitative properties of the synthesized materials. In the PL spectra, GO, GO-LP, and GO-LP/PMAM illustrate a narrow emission at 420 nm, when excited at 280 nm. By comparing the results, it could be concluded that the PL spectrum of GO-LP/PMAM compared to GO and GO-LP spectra in water become stronger which is mainly due to the formation and amplification of phenomenon such as internal and external transformations and intersystem transitions through the modification of GO. This higher PL property of prepared GO-LP/PMAM makes it potentially usable as a nanosensor for detecting various ions.

3.7. Fluorescence selectivity and competition experiments

Fluorescence selectivity experiments were designed and carried out in deionized water to investigate the fluorescence selectivity of nanosensor against various metal ions (Ag (II), Zn (II), Cd (II), Pb (II), Hg (II), Fe (II), Mn (II), Ni (II), Co (II), Cu (II)). As seen in Fig. 5, titration of different metal ions could not significantly change the fluorescence signal; however, Cu (II) led to a high quenching in the fluorescence signal. The fluorescence testing demonstrated that an interaction existed between metal ions and nanosensor that quenched the fluorescence behavior of nanosensor dependent on metal ions [17] (Scheme 2). Also, the fluorescence manner showed that the GO-LP/PMAM nanosensor could act as a selective fluorescent detector for Cu (II).

Competitive metal ion addition was performed to study the selectivity of GO-LP/MAM to sense Cu (II) in the presence of various metal ions *via* titration of an equimolar amount of Cu (II) to a solution of GO-LP/MAM and each metal ion. As shown by Fig. 6A, Ag (II) and Pb (II) led to a dramatic increase in the fluorescence intensity. However, absence of any obvious alteration in the fluorescence intensity after the addition of other metal ions indicated the great selectivity for Cu (II). The sensitivity of GO-LP/MAM toward Cu (II) was achieved by titration of GO-LP/MAM solution with various amounts of Cu (II).

Emissions of nanosensor were linearly decreased by increasing the Cu (II) concentration (Fig. 6B), which showed the capability of this manner for the detection of Cu (II) in the 0.25-2 mM range in aqueous media. Therefore, GO-LP/MAM could be potentially used as a nanosensor for the detection of Cu (II) through the presence of emission at 420 nm.

4. Conclusions

A novel nanosensor based on the modification of GO was synthesized *via* RAFT polymerization of MAM monomers onto the surface of GO. The proposed mechanism was presented for the modification of GO. The prepared nanosensor was confirmed by FT-IR, SEM, DLS, TGA, UV-Vis, and PL techniques. The fluorescence manner showed that the modified GO, GO-LP/PMAM nanosensor could act as a selective fluorescent detector for Cu (II) in the range of 0.25-2 mM (correlation coefficient R^2 0.9903). Results revealed that the modified GO *via* RAFT polymerization strategy could be employed for the sensing of Cu (II) ions from aqueous media as an effective nanosensor.

Declarations

Acknowledgments

The authors express their sincere gratitude to the University of Tabriz for providing financial support to this research.

Author Declarations

-Funding

No funding resources

-Conflicts of interest/Competing interests

The authors declare that they have no conflict of interest.

-Ethics approval

Not applicable

-Consent to participate

Not applicable

-Consent for publication

Not applicable

-Availability of data and material

Not applicable

-Code availability

Not applicable

-Authors' contributions

Mehdi Barzegarzadeh: Investigation, Software, Visualization, Resources

Mohammad Sadegh Amini-Fazl: Conceptualization, Methodology, Validation Writing - Original Draft, Supervision

Seyed Yasin Yazdi-Amirkhiz: Writing - Reviewing and Editing

References

1. Andryushina NS, Stroyuk OL, Dudarenko GV, Kuchmiy SY, Pokhodenko VD (2013) Photopolymerization of acrylamide induced by colloidal graphene oxide. *Journal of Photochemistry and Photobiology A: Chemistry* 256:1-6
2. Becerril HA, Mao J, Liu Z, Stoltenberg RM, Bao Z, Chen Y (2008) Evaluation of solution-processed reduced graphene oxide films as transparent conductors. *ACS nano* 2 (3):463-470
3. Botas C, Álvarez P, Blanco P, Granda M, Blanco C, Santamaría R, Romasanta LJ, Verdejo R, López-Manchado MA, Menéndez R (2013) Graphene materials with different structures prepared from the same graphite by the Hummers and Brodie methods. *Carbon* 65:156-164
4. Carter KP, Young AM, Palmer AE (2014) Fluorescent sensors for measuring metal ions in living systems. *Chemical reviews* 114 (8):4564-4601
5. Chen Y, Tan H-m (2006) Crosslinked carboxymethylchitosan-g-poly (acrylic acid) copolymer as a novel superabsorbent polymer. *Carbohydrate Research* 341 (7):887-896
6. Eftekhari-Sis B, Mirdoraghi S (2016) Graphene oxide-terpyridine conjugate: a highly selective colorimetric and sensitive fluorescence Nano-chemosensor for Fe²⁺ in aqueous media. *Nanochemistry Research* 1 (2):214-221
7. Ejeian F, Etedali P, Mansouri-Tehrani H-A, Soozanipour A, Low Z-X, Asadnia M, Taheri-Kafrani A, Razmjou A (2018) Biosensors for wastewater monitoring: A review. *Biosensors and Bioelectronics* 118:66-79
8. Gao X, Jang J, Nagase S (2009) Hydrazine and thermal reduction of graphene oxide: reaction mechanisms, product structures, and reaction design. *The Journal of Physical Chemistry C* 114 (2):832-842
9. Göde C, Yola ML, Yılmaz A, Atar N, Wang S (2017) A novel electrochemical sensor based on calixarene functionalized reduced graphene oxide: application to simultaneous determination of Fe (III), Cd (II) and Pb (II) ions. *Journal of colloid and interface science* 508:525-531

10. Grimm DM, Azarraga LV, Carreira LA, Susetyo W (1991) Continuous multiligand distribution model used to predict the stability constant of copper (II) metal complexation with humic material from fluorescence quenching data. *Environmental science & technology* 25 (8):1427-1431
11. Hua M, Wang C, Qian J, Wang K, Yang Z, Liu Q, Mao H, Wang K (2015) Preparation of graphene quantum dots based core-satellite hybrid spheres and their use as the ratiometric fluorescence probe for visual determination of mercury (II) ions. *Analytica chimica acta* 888:173-181
12. Javanbakht S, Pooresmaeil M, Namazi H (2019) Green one-pot synthesis of carboxymethylcellulose/Zn-based metal-organic framework/graphene oxide bio-nanocomposite as a nanocarrier for drug delivery system. *Carbohydrate polymers* 208:294-301
13. Jin T, Yin H, Easton CD, Seeber A, Hao X, Huang C, Zeng R (2019) New strategy of improving the dispersibility of acrylamide-functionalized graphene oxide in aqueous solution by RAFT copolymerization of acrylamide and acrylic acid. *European Polymer Journal* 117:148-158
14. Kickelbick G (2003) Concepts for the incorporation of inorganic building blocks into organic polymers on a nanoscale. *Progress in polymer science* 28 (1):83-114
15. Løvstad RA (2004) A kinetic study on the distribution of Cu (II)-ions between albumin and transferrin. *BioMetals* 17 (2):111-113
16. Lu L-Q, Tan T, Tian X-K, Li Y, Deng P (2017) Visual and sensitive fluorescent sensing for ultratrace mercury ions by perovskite quantum dots. *Analytica Chimica Acta* 986:109-114
17. Nath P, Arun RK, Chanda N (2015) Smart gold nanosensor for easy sensing of lead and copper ions in solution and using paper strips. *Rsc Advances* 5 (84):69024-69031
18. Prucker O, Rühle J (1998) Synthesis of poly (styrene) monolayers attached to high surface area silica gels through self-assembled monolayers of azo initiators. *Macromolecules* 31 (3):592-601
19. Ryan DK, Weber JH (1982) Copper (II) complexing capacities of natural waters by fluorescence quenching. *Environmental Science & Technology* 16 (12):866-872
20. Ryan DK, Weber JH (1982) Fluorescence quenching titration for determination of complexing capacities and stability constants of fulvic acid. *Analytical Chemistry* 54 (6):986-990
21. Tapiero H, Townsend Dá, Tew K (2003) Trace elements in human physiology and pathology. *Copper. Biomedicine & pharmacotherapy* 57 (9):386-398
22. Tolessa T, Tan Z-Q, Liu J-F (2018) Hydride generation coupled with thioglycolic acid coated gold nanoparticles as simple and sensitive headspace colorimetric assay for visual detection of Sb (III). *Analytica Chimica Acta* 1004:67-73
23. Tran Y, Auroy P (2001) Synthesis of poly (styrene sulfonate) brushes. *Journal of the American Chemical Society* 123 (16):3644-3654
24. Ullah N, Mansha M, Khan I, Qurashi A (2018) Nanomaterial-based optical chemical sensors for the detection of heavy metals in water: Recent advances and challenges. *TrAC Trends in Analytical Chemistry* 100:155-166

25. Xu H, Suslick KS (2011) Sonochemical preparation of functionalized graphenes. *Journal of the American Chemical Society* 133 (24):9148-9151
26. Zhang H, Zhang H, Aldabahi A, Zuo X, Fan C, Mi X (2017) Fluorescent biosensors enabled by graphene and graphene oxide. *Biosensors and Bioelectronics* 89:96-106
27. Zhang J, Wang Q, Wang A (2007) Synthesis and characterization of chitosan-g-poly (acrylic acid)/attapulgit superabsorbent composites. *Carbohydrate polymers* 68 (2):367-374
28. Zheng P, Wu N (2017) Fluorescence and sensing applications of graphene oxide and graphene quantum dots: a review. *Chemistry–An Asian Journal* 12 (18):2343-2353

Figures

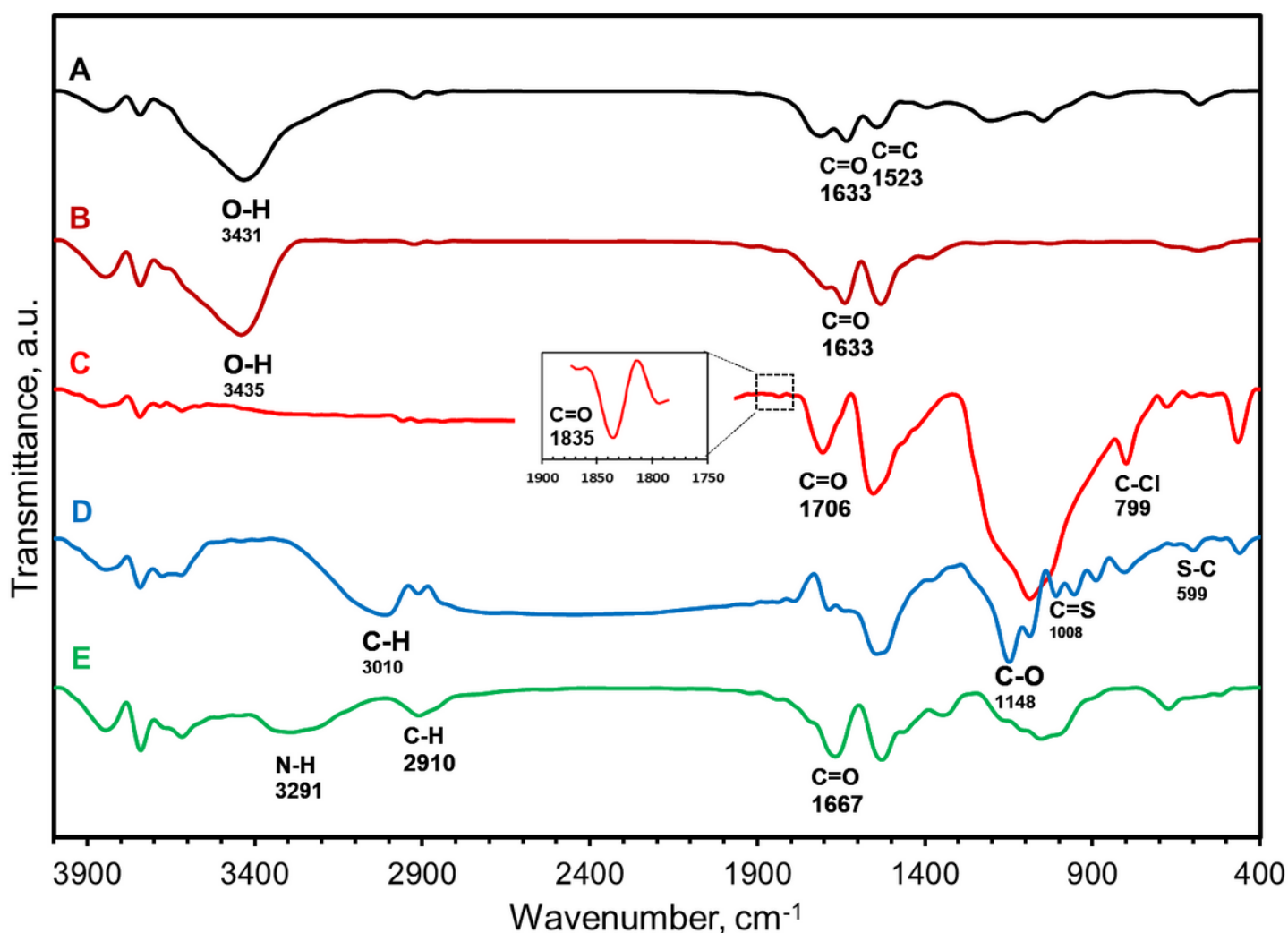


Figure 1

FT-IR spectra of the GO (A), GO-LP (B), GO-LP-COCl (C), GO-LP-RAFT (D), and GO-LP/PMAM (E).

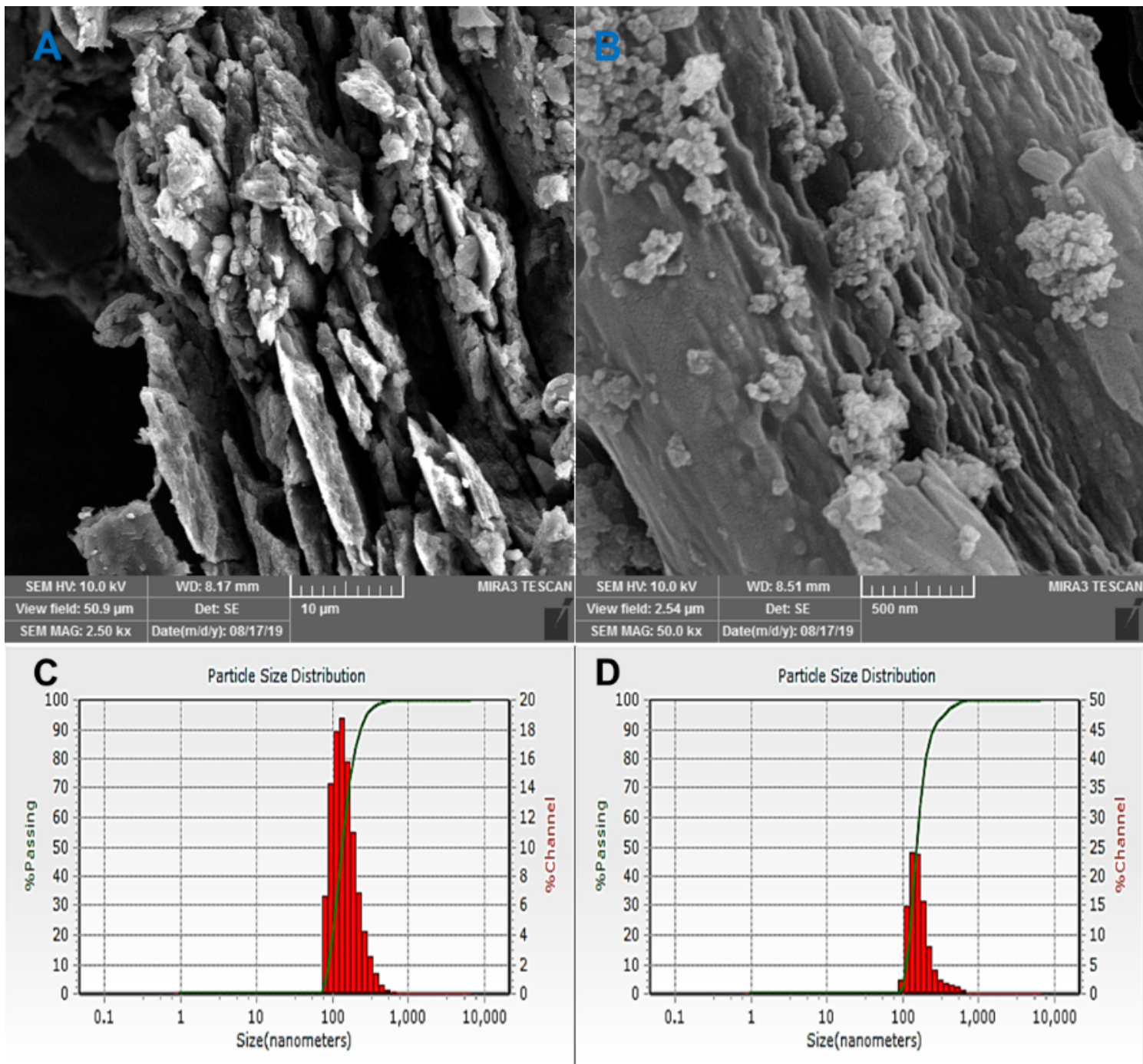


Figure 2

SEM images of the GO (A), GO-LP/PMAM (B), and DLS spectra for GO (C) and GO-LP/PMAM (D).

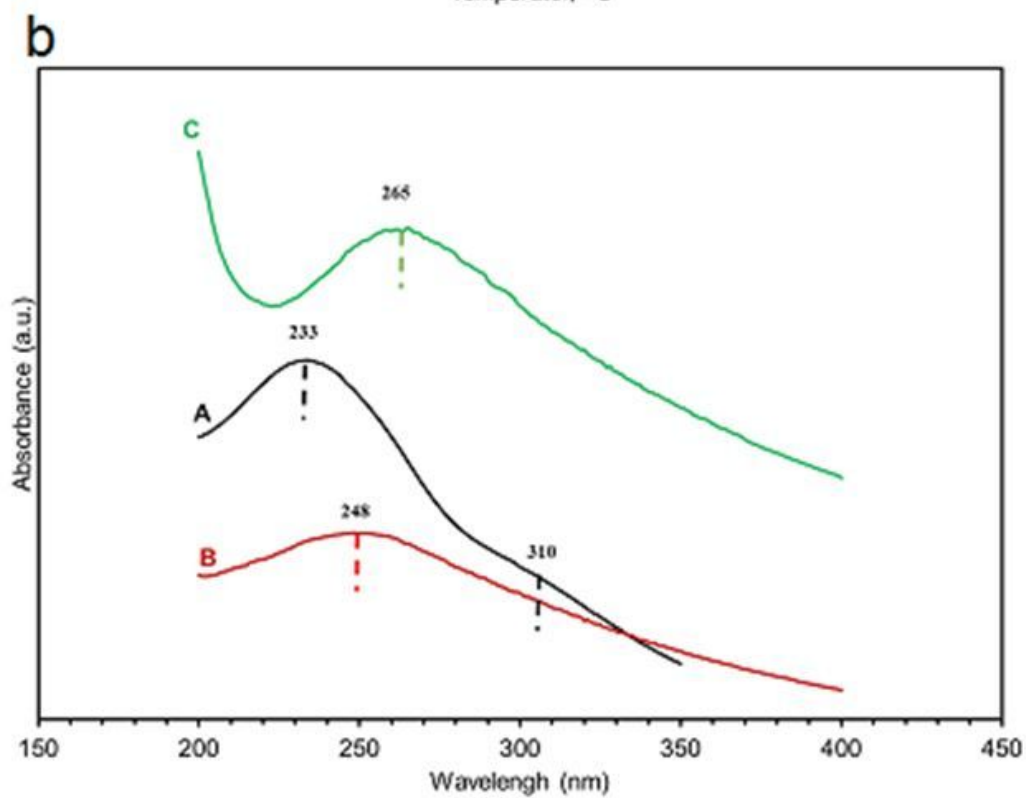
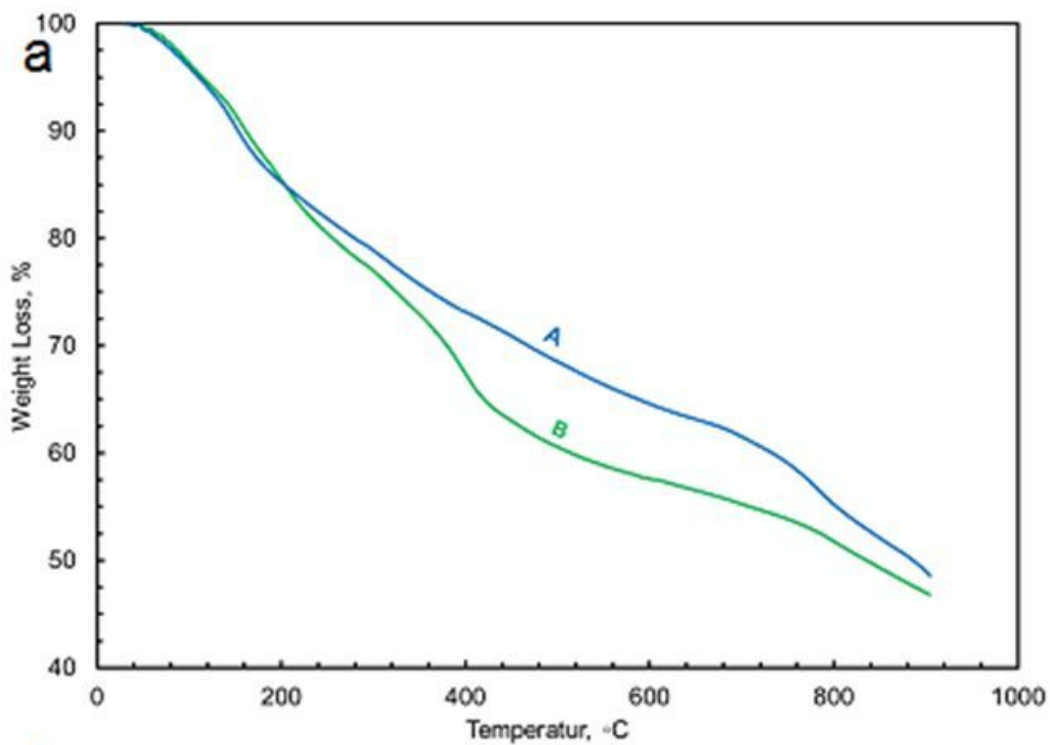


Figure 3

a) TGA curves of GO-LP-RAFT (A) and GO-LP/PMAM (B). b) UV-Vis absorption of GO (A), GO-LP (B) and GO-LP/PMAM (C)

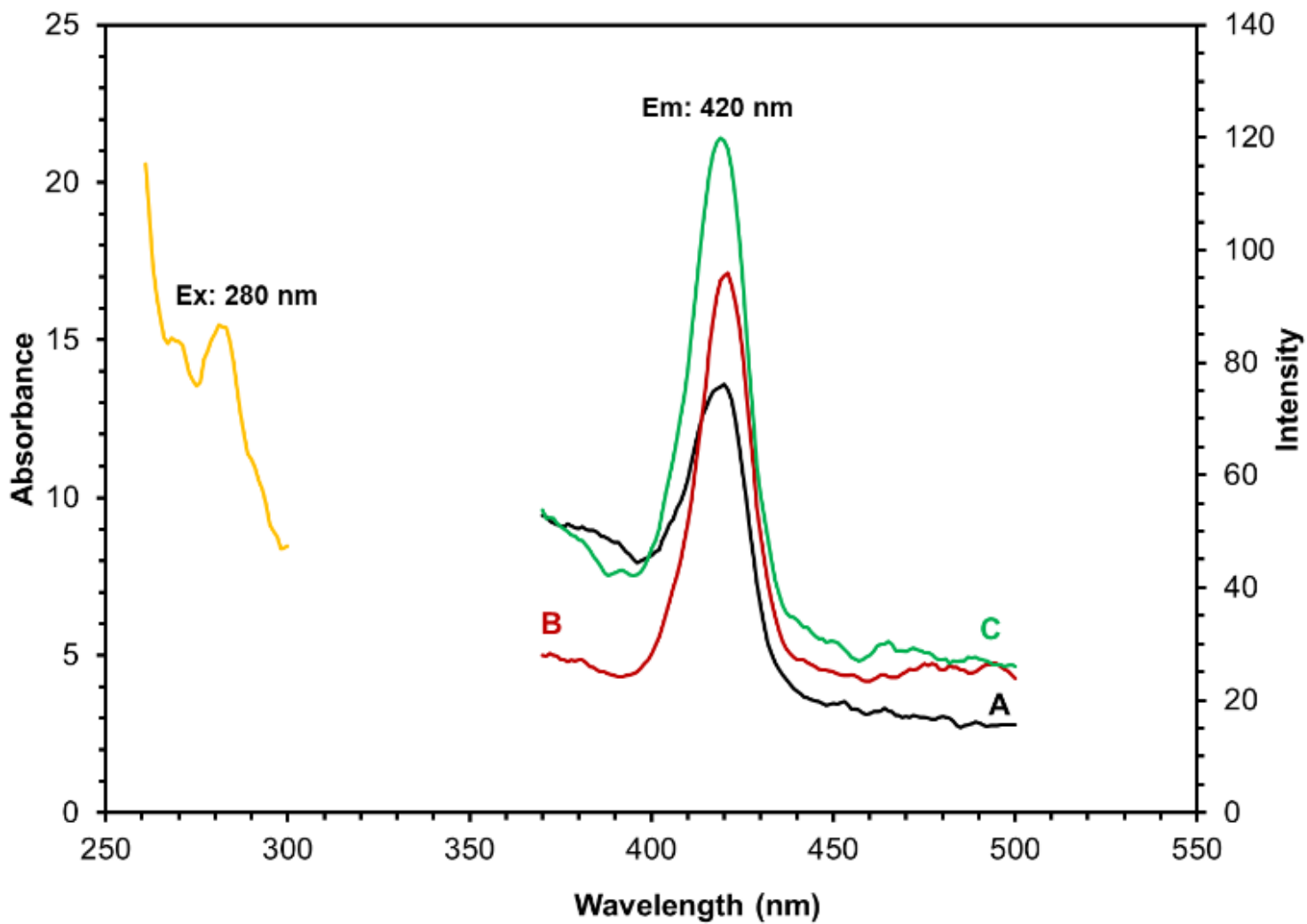


Figure 4

PL spectra for GO (A), GO-LP (B), and GO-LP/PMAM (C) with 4 mg/mL concentration 3.7. Fluorescence selectivity and competition experiments

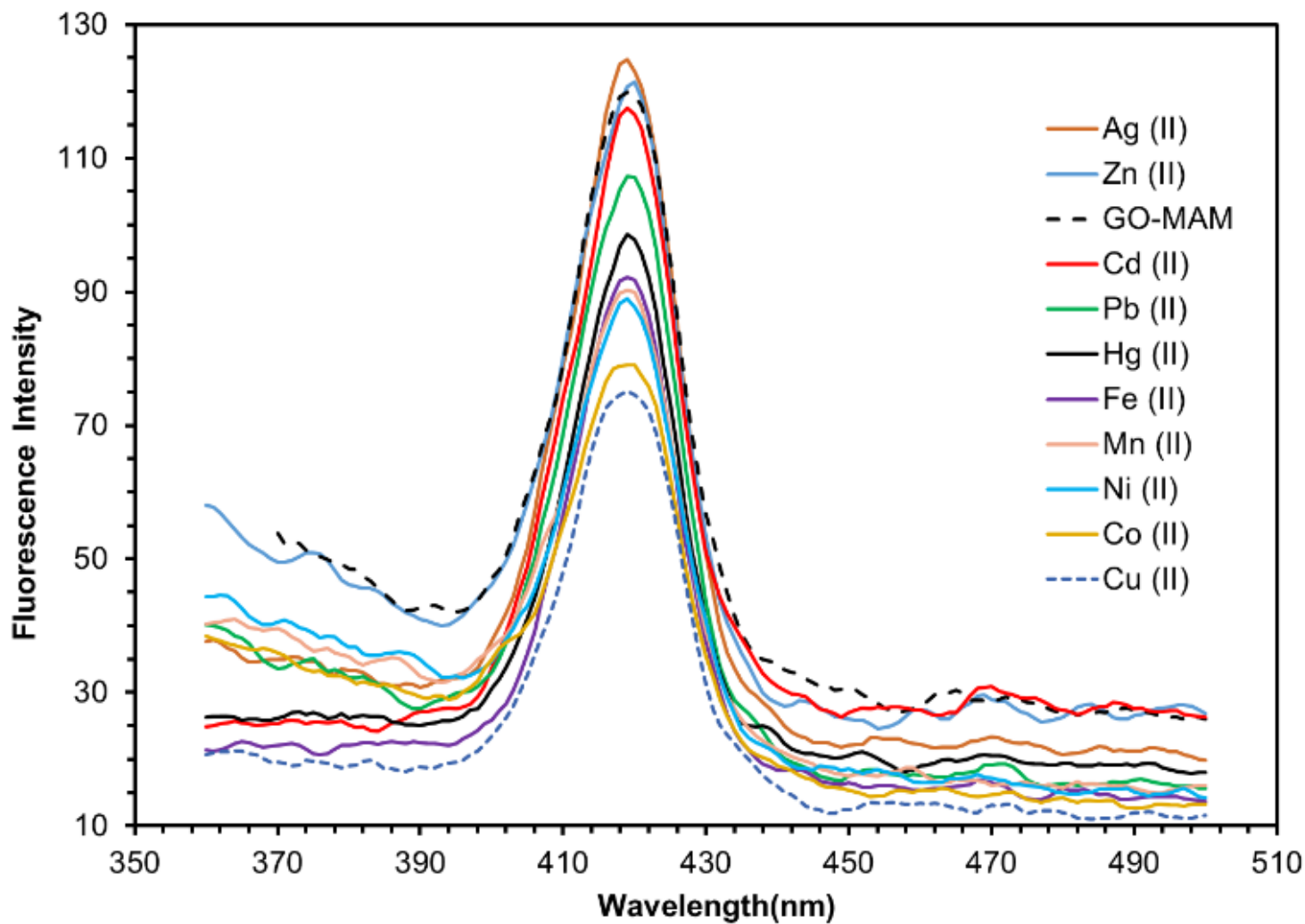


Figure 5

PL spectra of GO-LP/PMAM (excited at 280 nm) in the presence of metal ions

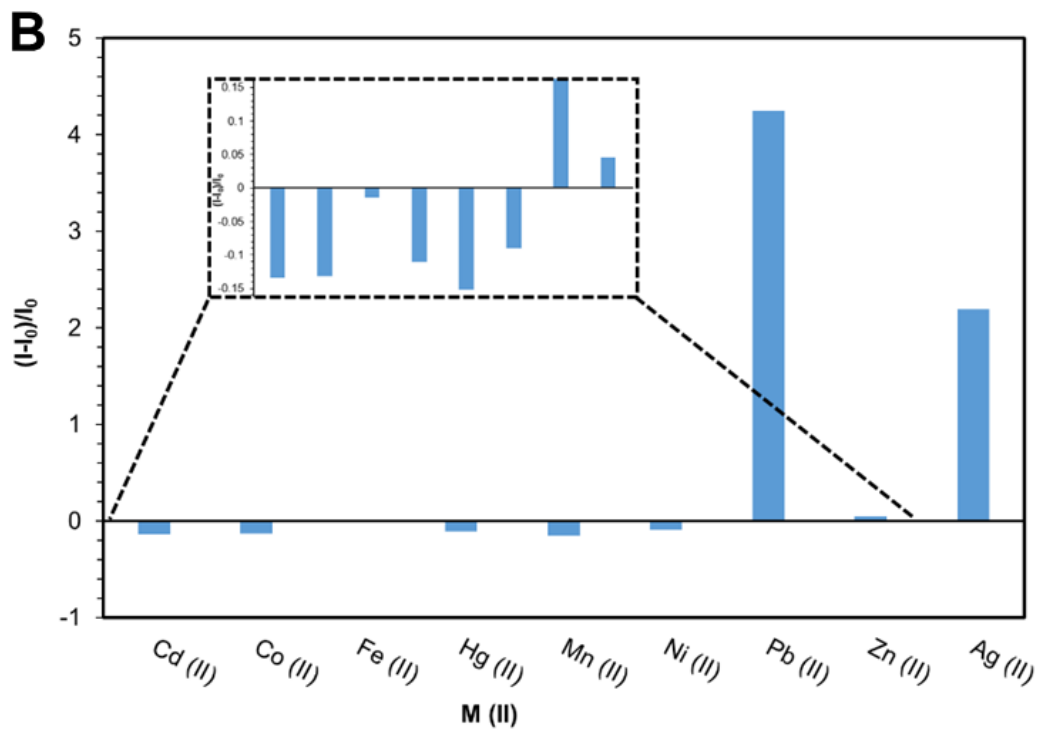
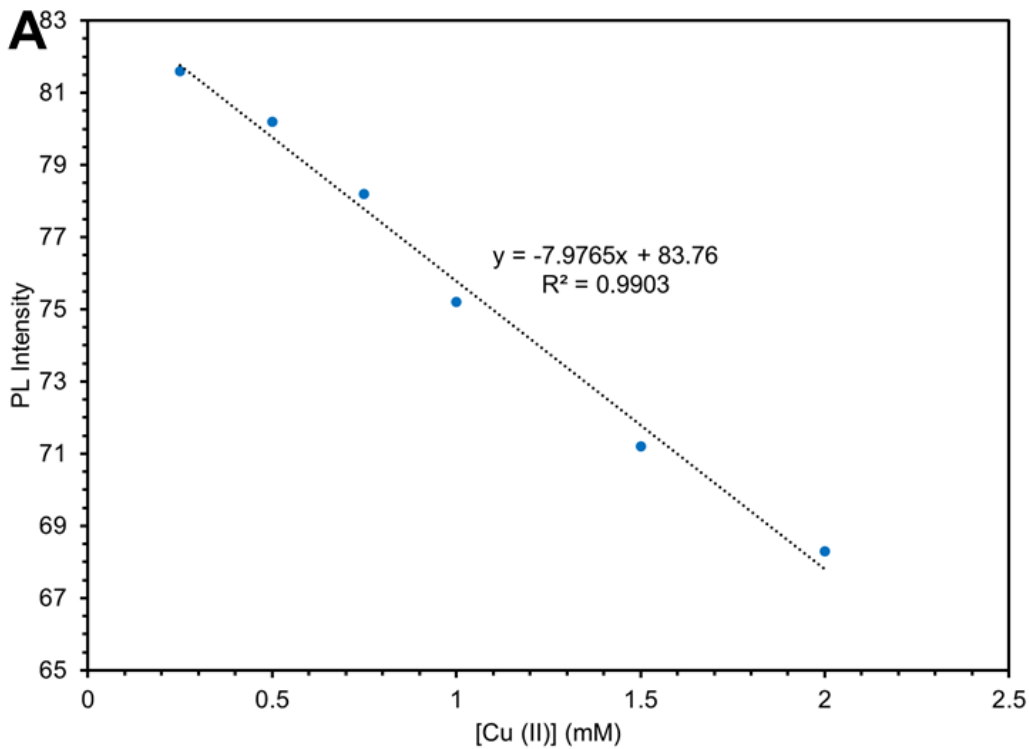


Figure 6

Calibration PL spectra of GO-LP/PMAM against titration with different Cu (II) concentration (A); Fluorescence intensity changes ($I-I_0/I_0$) of the nanosensor in the presence of the equimolar amount of each metal ion; Inset: the enlarged area (B)

Supplementary Files

This is a list of supplementary files associated with this preprint. Click to download.

- [scheme1.jpg](#)
- [scheme2.jpg](#)